Effective (Cuo) Nanoparticles with Crocus Sativus Prepared by Green Synthesis of S. Aureus and S.Epidermidis Activity

Noor Al-Huda R. Ali[1], Majid H. Hassouni[2]
[1], [2]Physics Department / Collage of Education / Mustansiriyah University/ Iraq.
*Email: nooralhuda199138@gmail.com
Email: majidhamid1965@uomustnsiriyah.edu.iq

Abstract
Due to their electric, optical, photonic, catalytic, and antimicrobial properties, copper oxide nanoparticles (CuO NPs) have received a great deal of attention. using plants *Crocus Sativus*. A green, non-toxic, and economical method of creating nanostructured materials is through biosynthesis. So, the purpose of this work is to present an updated overview of the primary green synthesis process of CuO NPs utilizing Crocus extract, as well as studies on its characterization and antibacterial activity. A UV-Visible (UV-Vis) spectrophotometer that detected surface Plasmon resonance at 308 nm was used to study the reaction's kinetics. *Staphylococcus aureus* and *Streptococcus epidermoid* are two human pathogens that the CuO NPs exhibit antibacterial efficacy against, with average zones of inhibition of 20 mm and 17 mm, respectively. In order to acquire considerably active antibacterial material, the current study demonstrates a practical application of Crocus Sativus extract was used as a reducing agent in the effective green synthesis of CuO NPs.

Keywords: Nanoparticles, Copper oxide, Crocus, Green synthesis, FTIR, XRD, PL and Antibacterial

1. Introduction

Nanomaterials research is now the most alluring, well-liked, and comforting area [1-2]. Many experts, including chemists, metallurgists, physicists, material scientists, biologists, etc., are conducting extensive research in this area because of the remarkable diversity of features that nanomaterials exhibit when compared to their bulk counterparts. [3,4]. In recent years, metal and metal oxide nanoparticles have significantly improved sensing, imaging, diagnosis, and therapy in biomedicine. The three metals that are used the most frequently today are silver, copper, and gold. a cheap, high-yielding substance that can exploited in biomedical and environmental remediation applications among these metal nanoparticles is copper [5]. are well-known to us and show certain characteristics and uses. The metal oxide nanoparticles are the ones that are advancing the fastest among all of them because of how simple they are to make, how little they are, how much surface area they have, how well they function, and how many different things you can do with them. Applications for electron transistors, electro-catalysts, gas sensors, pigments, and solar cells are just a few. [6] wastewater treatment, electro-chemical sensors [7, 8] Different mechanisms , such as physical, chemical, and biological ones, can produce these nanostructures. Although physical and chemical processes generate a large number of nanoparticles, they are not preferred due to the use of hazardous materials, high costs, and energy needs. Green methodologies have emerged to address the limitations of physical and chemical processes. Utilizing natural and organic materials is a component of the green synthesis process. The use of a number of biological agents, such as bacteria, can achieve this goal [9,10] However, these procedures can occasionally be cumbersome, sluggish, and necessitate the use of expensive machinery, specialized chemicals, poisonous capping agents, high temperatures, etc. These procedures are not safe for the environment and are not used to create metal oxide nanoparticles since they employ potent and hazardous chemicals. Therefore, we opted to employ an easy, quick, affordable, environmentally benign technology like the green production of metal oxide nanoparticles by flower extract. The abundance and diversity of flora are the key benefits of this approach. Typically, plants include phytochemicals such aldehydes, ketones, flavonoids, and phenols that function as reducing agents and transform metal salts into metal oxide nanoparticles. dispersion substances for alloys, etc. In this study, we will investigate Effective (CuO) Nanoparticles with Crocus Sativus extract Prepared by Green Synthesis of *S.aureus* and *S.epidermidis* Activity are two forms of positive bacteria. We are familiar with a variety of metal oxide CuO, ZnO, TiO2, Fe2O3, Al2O3, MgO, AgO, CeO2, and ZrO2. [11] The reason we chose Botanical Extract is because Plants have elements that can function as chelating, capping, stabilizing, and reducing agents for the synthesis of nanoparticles. High reduction potential noble metal nanoparticles have been successfully created [12].CuO nanoparticles, however, stand out among all other nanomaterials because they have a variety of useful features and uses. As a result, we chose to make CuO nanoparticles using an extract of the Crocus sativus (saffron) flower. Saffron crocus is the common name for the Crocus Sativus [13], and it is a type of flowering plant that is a member of the Iridaceae (iris) family. Typically, the Mediterranean, East Asia, and Irano-Turanian Region are where Crocus sativus is farmed [14]. The stigma is the only component of the plant that may be used; the rest is wasted material. Seventy thousand hectares of saffron plantations are located in Iran. The location that produces the most saffron is the South Khorasan Province. The petals of saffron, which contain precious colors known as anthocyanins, are discarded after the stigmas are separated. The substances known as anthocyanins are responsible for the color of saffron petals. The flavonoid family of natural substances and secondary metabolites includes anthocyanins [15,16]. Saffron is a spice that grows inside the blossom As shown in the figure(1)and is used in many cultures as a flavor in food and tea preparation. Asthma, cough, whooping cough, sleeplessness, Alzheimer's disease, cancer, atherosclerosis, intestinal gas, depression, hemoptysis, heartburn, and dry skin are other conditions that are treated with saffron. [17] Saffron petals contain a number of different substances. Flavonols like kaempferol and From saffron petals, quercetin, isorhamnetin, and anthocyanins like delphinidin, petunidin, and Maldivian are extracted [18]. The copper oxide (CuO) nanoparticles are a brownish-black powder with good electrical conductivity, exceptional ductility, high hardness, and high luminous efficiency, among other characteristics. [19]. CuO nanoparticles are employed as superconducting, thermo-electric, burning rate catalysts in magnetic storage, photothermal, photoconductive, and rocket propellant materials due to their exceptional capabilities. When they are small, CuO nanoparticles typically have semiconducting properties, but as they become larger, they gradually change their behavior [20] Creating CuO NPs with this method is the primary goal of this work. using crocus extract and evaluating its antibacterial performance on a sample of bacteria.

Fig. Shows (1) Crocus Sativus blossom

Experimental work

The Crocus plant, which was used in the synthesis, was obtained from Iraqi local markets and verified by the herbarium of the Iraqi Ministry of Health. It was thoroughly cleaned with double-distilled water before use. Deionized water 0.1L distal water was added along with two grams of freshly cut Crocus Sativus (saffron) flowers. We boiled the flower-water mixture at 80 °C for 15 to 20 minutes to produce a strong, red-colored solution. The flower extract solution should then be cooled to room temperature (roughly 25 °C), filtered through all-purpose filter paper, and centrifuged to remove any impurities, yielding a clear red solution. All throughout the experiment, a small amount of the flower extract was used to prepare the CuO nanoparticles, and aliquots were stored at 5 °C temperature for future use. The figure (2) shows the stages of Crocus extract preparation:

Fig.2: shows the stages of Crocus preparation (a) deionized distal water (b) Crocus Sativus with deionized distal water (c) Crocus Sativus extract.

Preparation of CuO nanoparticles

To make 1M of copper oxide, copper nitrate Cu $(NO3)_2$ (1.8 g) (Molar mass=187.56 g/mol) was added to 0.1L of distilled water. For one hour of aiming, The device (Hot Plate and Magnetic Stirrer) is placed with the mixture in it. at 60 0 C will A blue solution is formed. Then, combine with 5 ml of the plant extract (Crocus) solution to create. solution that represents the CuO Crocus mix, and then incubate for an additional hour at 60°C. Over time, the solution's color turns from blue to Green As shown in the figure (2) on the left .that the progressive alteration in color is caused by the formation of CuO NPs. The optical absorption spectra of Copper oxide NPs were calculated using a UV-Vis Spectrophotometer was used by Crocus to examine the shape of CuO nanoparticles (AFM). The functional groups of the produced extracts were investigated using an FT-IR (Shimadzu / 84005) [7] To ascertain the crystal structure of the particles, X-ray diffraction (XRD) was employed The antibacterial effectiveness of CuO NPS was tested against *Staphylococcus aureus* and *Staphylococcus epidermidis* using advanced diffusion agar techniques.

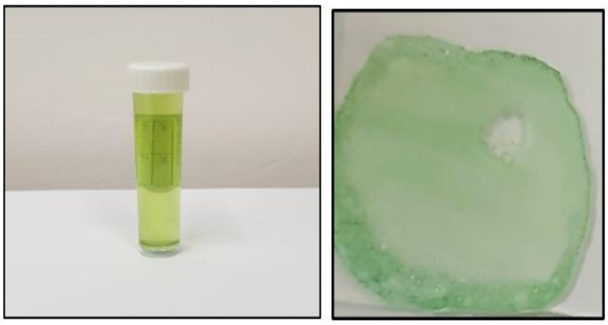

Fig.3: CuO NPs on the left and CuO thin film prepared by drop casting method on right

2. Results and discussion

Structural analysis of CuO and nanoparticles by XRD

Figure 4 shows the XRD diffraction pattern of biosynthesized Cuo nanostructure film formed on glass substrate using the drop-casting method with 3 drops (each drop equaling 100 l). The reflections (110), (311), (111), and (220) are easily visible and closely match the reference patterns for CuO According To Card Number (JCPDS-05-0661and JCPDS Card Number 45- 0937) From the Debye-Scherrer formula was calculated the size of the biosynthesized CuO nanostructure crystallites to :

$D = k\boldsymbol{\lambda} / \boldsymbol{\beta} \ \boldsymbol{cos\theta}$ (1)

where D = average crystallite size, K = A constant equal to 0.94, λ = the wavelength of X-ray radiation (0.154 nm).The XRD analysis results of pure Cuo Nps produced using a green production strategy are shown in Figure 4. Seven 2 Figures Were Vividly Noticed Ranging from 30 To 80 According To The Findings Of The Film X-Ray Examination. Identifying the type of the generated nanoparticles requires a thorough X-ray examination of the film It displayed various diffraction angles as shown in Table 1, with the largest crystal size of Cu equaling 85.13 and the smallest crystal size of Cu2O (13.69) as shown in the table (1). These matched well with the standard Peaks Card Number because the Diffraction Peaks Are Indexed to Hexagonal Structure (JCPDS-05-0661and JCPDS Card Number 45- 0937).

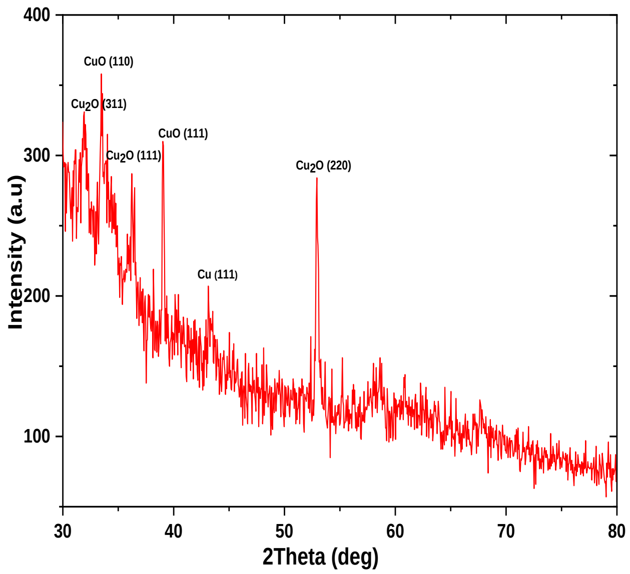

Fig. 4: XRD diffraction pattern of CuO nanoparticles prepared from Crocus Sativus (Saffron) flower extract

Table. 1: The values of theFWHM, crystallite size

2 Theta (deg)	D (nm)	FWHM (deg)	Strain*10-4	hkl	Materials
31.9	**13.69**	0.010	25.29	(311)	Cu2o
32.49	20.58	0.0070	16.83	(110)	Cuo
36.2	41.57	0.0035	8.33	(111)	Cu2o
39.18	27.96	0.0052	12.38	(111)	Cuo
43.52	**85.13**	0.0017	4.070	(111)	Cu
52.95	35.34	0.0043	9.803	(220)	Cu2o

Atomic Force Microscope (AFM) Results:

Fig. 5 shows a picture of a CuO thin film in three dimensions that was created at substrate temperature. With each columnar grain extending upward, the grains were evenly dispersed. The average grain size of the pore, as determined by AFM analysis, was found to be approximately 11.89 nm, with an RMS Roughness of 2.62 nm and a Roughness Average of 24.55 nm As Shown in the Table 2

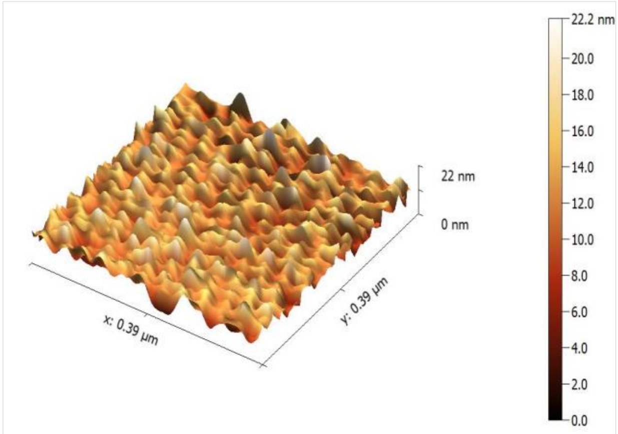

Fig. 5: 3D Image of AFM (Green synthesis)

Table. 2: The parameter of copper oxide surface

Average value	11.89 nm
Minimum	0.00 nm
Maximum	24.55nm
Median	11.89 nm
Ra	2.06 nm
Rms	2.62 nm
Rms (grain-wise)	2.62 nm

C. FFTIR spectrum

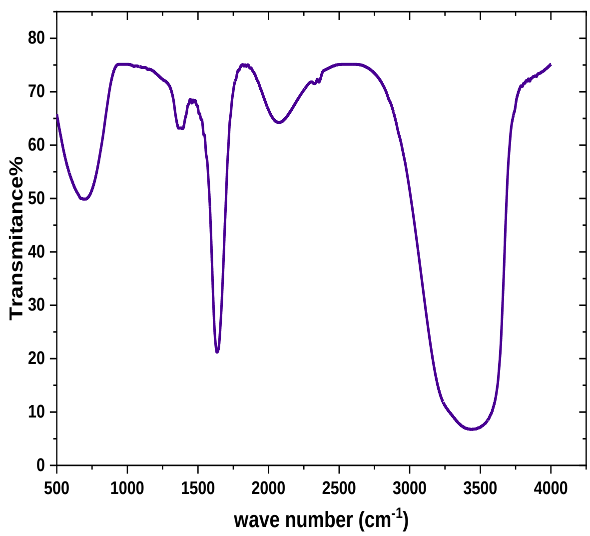

Fig. 6: The FTIR spectra of CuO, prepared by Crocus Sativus (Saffron) flower extract.

The FTIR spectra of biosynthesized CuO nanoparticles is shown in Figure 6. Broad absorption bands between 2750 and 3500 cm^{-1} can be seen in the FTIR spectra of CuO nanoparticles, which are primarily due to O-H and C-O groups. The surface hydroxyl groups of adsorbed water molecules' O-H stretching vibration were found to produce a strong wide band in the region of 3200-3550 cm1 [21]. This develops because materials made of nanocrystal lines with a high surface-to-volume ratio absorb a lot of moisture This peak can be attributed to the CuO nanoparticles' high surface-to-volume ratio nanocrystal line structure. The tiny band at around 2100 cm1 is caused by the stretching vibration of O=C=O. The C=C bending vibration and the anticipated production of bidentate ligand coordination between C-O and Cu (II) of CuO are the causes of the strong absorption band at about 1640 cm^{-1} [22]. The C-H bond of an alkane's C-H bond is principally responsible for the steep peak at 1350 cm^{-1}. The Cuo bond's aromatic bending vibration is what causes the peak to rise to 667. The IR bands in the places listed above provide confirmation that.

d. UV–visible spectroscopy

Fig.7(a) depicted the optical characteristics of CuO nanoparticles synthesized from Crocus sativus (saffron) flower extract were investigated using the UV-visible spectroscopy. shows the CuO absorption as a function of wavelength after being produced via the green synthesis According to the results, translucence qualities are sufficient in the spectral region of 200 nm to 1100 nm and dramatically increase with increasing absorbed particle size width. Along with that, It has a distinct peak at 240. Analyzing optical properties was done to use a UV-Visible spectrometer of type UV-2610 produced in the UK by Biotech Engineering Management Company. Fig. 7(a) shows the optical absorption characteristics of Cu-oxide nanoparticles; the absorption spectra become narrower with increasing wavelength. It discovered a peak with a wavelength of 308 nm. This is known as a Plasmon resonance and is attributable to the creation of copper oxide in solution. CuO NPs had a high degree of transparency in the visible and infrared spectrum, and their highest absorption was around 1.17 at 200 nm [23]

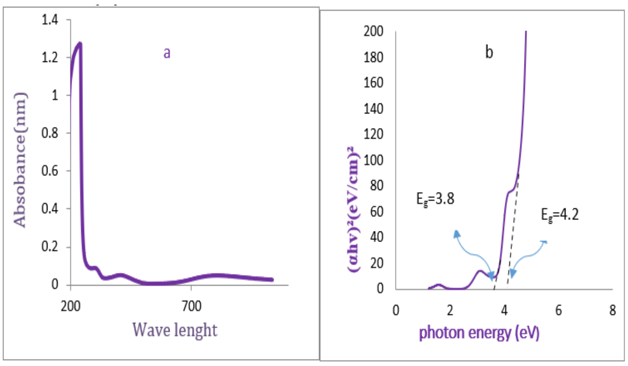

Fig. 7: a UV–Vis spectra of Cuo NPs sample prepared by Crocus plant extract and (b)$(\alpha hv)^2$ versus hv For Cuo NPs

Fig.7(b) On the Right displays a graph of $(\alpha hv)^2$ vs photon energy (hv) that From Tauc's Relation calculated the band gap of Copper oxide was 3.8 eV There is an increase in the value of the band gap to 4.2 which may be attributed to the quantum size effect. the optical spectra of nanostructured systems are affected by the quantum size effect, which causes a blue shift. The band gap of a bulk semiconductor moves to a higher energy level as a result of the quantum size effect. [24] The presence of the mono-, binary-, and tri-elements of copper oxide may be the cause of the two energy gaps.

e. Photoluminescence (PL):

can be used to analyze the fluorescence characteristics of a material. A material's molecular composition can be determined using fluorescence spectra., it is observed that Emission spectrum at a wavelength 320 nm As shown in the figure(8) the biosynthesized CuO Nanomaterials exhibit fluorescence when the energy gap is present 3.8ev This is because phytochemicals are present. (Crocus plant extract) attached to the CuO nanoparticles Compared to chemically produced CuO nanoparticles, biologically produced copper oxide nanoparticles have a higher PL intensity according to Muthuvel et al. [25]

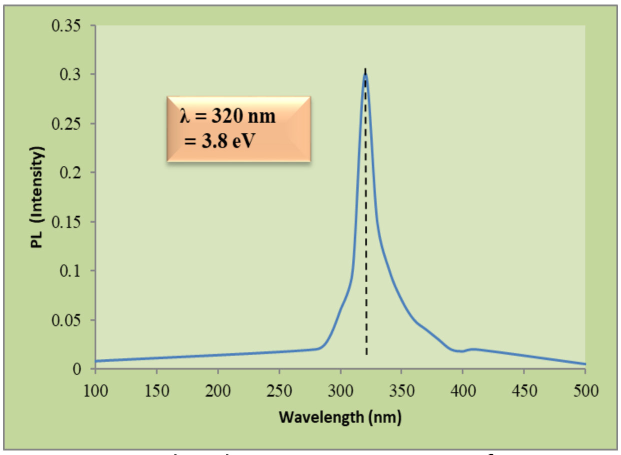

Fig.8: Photoluminescence spectra of cuo

Antibacterial application:

Plant synthesis of Cuo NPs showed antibacterial activity using the agar well diffusion method, as shown in figure 9. The outcomes made obvious which Cuo NPs were effective against the bacterial isolates listed in Table 3 in the results. It found the inhibition zone diameter of *S. aureus* (20 mm) and *S. epidermidis* bacterial isolates (17 mm) The concentration of the antibacterial agent, the kind of bacteria, the sample surface area, and the shape and size of NPs were some of the variables that affected the inhibitory zone Due to electrostatic forces, bacteria charges and nanoparticles that are the opposite are responsible for their adherence and bioactivity. It makes sense to say that the surface area that is open to contact determines how tightly nanoparticles are bound to bacteria. In comparison to larger particles, nanoparticles have a larger available surface area for interactions, which boosts their ability to kill bacteria. As a result, they cause cytotoxicity in microorganisms.[26] Changes in the membrane's morphology brought about a significant increase in permeability after exposure to nanoparticles, which interfered with proper transport through the plasma membrane and rendered bacterial cells unable to control. trafficking through the plasma membrane, ultimately leading to cell death.[27] Heavy metals attach to protein molecules and trigger harmful reactions with proteins [28]. Moreover, heavy metals aggressively interact with crucial enzymes' thiol groups, leaving them inactive. [29]. As a result of the slow release of membrane proteins and LPS molecules during metal depletion, bacteria's outer membrane develops pits of varying sizes. [30]

Table. 3: inhibition Zone rate		
Bacterial isolate	*S.aureus*	*S.epidermidis*
Inhibition zone rate	20 (mm)	17(mm)

Fig.9 Images of inhibition zone of bacteria

3. Conclusion

In this work, we succeed in preparation Cuo nanoparticles by green synthesis using Crocus extract. The all results was in nanoscale In this study The approach is straightforward and easy to use, and morphological observations have supported its validity for the synthesis of nanoparticles, which is why we believe it to be a viable method. XRD The nanoparticles' examination revealed an average size 37.3.2 nm in addition to an lysis Atomic Force Microscope (AFM) Results The average grain size of the pore, as determined by AFM analysis, was found to be approximately 11.89 nm, with an RMS Roughness of 2.62 nm. FTIR results supported the occurrence of Cuo NPs compounds from plant extract. this is indicates the effectiveness of green synthesis to form nanoparticles. The increasing use of nanoparticles in medicine has caused an increase in studies looking into their possible antibacterial actions, where in this work, the findings reveal that Cuo nanoparticles can prevent the growth gram positive bacteria (*Streptococcus epidermidis and Staphylococcus aureus)* The results indicate it can be used in other biological applications and even in physical applications.

References

Manjunatha, J. G., Deraman, M., Basri, N. H., & Talib, I. A. (2018). Fabrication of poly (Solid Red A) modified carbon nano tube paste electrode and its application for simultaneous determination of epinephrine, uric acid and ascorbic acid. *Arabian journal of chemistry*, *11*(2), 149-158.

, J.G. Manjunatha, M. Deraman, N.H. Basri, N.S.M. Nor I.A. Talib, N. Ataollahi, C. R. Chim. 17, 465 (2014)

Shashanka, R., Chaira, D., & Swamy, B. K. (2015). Electrocatalytic response of duplex and yittria dispersed duplex stainless steel modified carbon paste electrode in detecting folic acid using cyclic voltammetry. *Int. J. Electrochem. Sci*, *10*, 5586-5598.

Tigari, G., Manjunatha, J. G., Raril, C., & Hareesha, N. (2019). Determination of riboflavin at carbon nanotube paste electrodes modified with an anionic surfactant. *ChemistrySelect*, *4*(7), 2168-2173.

Honary, S., Barabadi, H., Gharaei-Fathabad, E., & Naghibi, F. (2012). Green synthesis of copper oxide nanoparticles using Penicillium aurantiogriseum, Penicillium citrinum and Penicillium waksmanii. *Dig J Nanomater Bios*, *7*(3), 999-1005.

Vinay, M. M., & Nayaka, Y. A. (2019). Iron oxide (Fe2O3) nanoparticles modified carbon paste electrode as an advanced material for electrochemical investigation of paracetamol and dopamine. *Journal of Science: Advanced Materials and Devices*, *4*(3), 442-450.

Manjunatha, J. G., Swamy, B. K., Deraman, M., & Mamatha, G. P. (2013). Simultaneous determination of ascorbic acid, dopamine and uric acid at poly (aniline blue) modified carbon paste electrode: a cyclic voltammetric study. *Int. J. Pharm. Pharm. Sci*, *5*, 355-362.

Manjunatha, J. G., Swamy, B. K., Shreenivas, M. T., & Mamatha, G. P. (2012). Selective determination of dopamine in the presence of ascorbic acid using a poly (nicotinic acid) modified carbon paste electrode. *Anal Bioanal Electrochem*, *4*(3), 225-37.

Abdella, A., Mazeed, T. E. S., El-Baz, A. F., & Yang, S. T. (2016). Production of β-glucosidase from wheat bran and glycerol by Aspergillus niger in stirred tank and rotating fibrous bed bioreactors. *Process Biochemistry*, *51*(10), 1331-1337.

Saif Hasan, S., Singh, S., Parikh, R. Y., Dharne, M. S., Patole, M. S., Prasad, B. L. V., & Shouche, Y. S. (2008). Bacterial synthesis of copper/copper oxide nanoparticles. Journal of nanoscience and nanotechnology, 8(6), 3191-3196.

Laurent, S., Boutry, S., Mahieu, I., Elst, L. V., & Muller, R. N. (2009). Iron oxide-based MR contrast agents: from chemistry to cell labeling. *Current medicinal chemistry*, *16*(35), 4712-4727.

Suresh, Y., Annapurna, S., Bhikshamaiah, G., & Singh, A. K. (2014). Copper nanoparticles: green synthesis and characterization. *International Journal of Scientific & Engineering Research*, *5*(3), 156-160.

United States Department of Agriculture (USDA), Agricultural Research Service, National Plant Germplasm System. Germplasm Resources Information Network (GRIN-Taxonomy). National Germplasm Resources Laboratory, Beltsville, Maryland (2020) https ://npgsw eb.ars-grin.gov/gring lobal /taxon omyde tail. aspx?id=12265

M. Kafi, A. Koocheki, M.H. Rashed, M. Nassiri, *Saffron (Crocus sativus) production and processing*, 1st edn. (Science Publishers, Singapore, 2006).

Wang, E., Yin, Y., Xu, C., & Liu, J. (2014). Isolation of high-purity anthocyanin mixtures and monomers from blueberries using combined chromatographic techniques. *Journal of Chromatography A, 1327* , 39-48.

Khazaei, K. M., Jafari, S. M., Ghorbani, M., & Kakhki, A. H. (2014). Application of maltodextrin and gum Arabic in microencapsulation of saffron petal's anthocyanins and evaluating their storage stability and color. *Carbohydrate polymers, 105*, 57-62.

Saffron, MedicineNet, https :// www. medic nenet.com /saffron/ supplement s-vitamins.htm

Goupy, P., Vian, M. A., Chemat, F., & Caris-Veyrat, C. (2013). Identification and quantification of flavonols, anthocyanins and lutein diesters in tepals of Crocus sativus by ultra performance liquid chromatography coupled to diode array and ion trap mass spectrometry detections. *Industrial crops and products*, *44*, 496-510.

AZoNano, Copper Oxide (CuO) Nanoparticles-Properties, Applications, 9th May (2013).

Rajendrachari, S., Kamacı, Y., Taş, R., Ceylan, Y., Bülbül, A. S., Uzun, O., & Karaoğlanlı, A. C. (2019). Antimicrobial investigation of CuO and ZnO nanoparticles prepared by a rapid combustion method. *Physical chemistry research*, *7*(4), 799-812.

Halder, A. K., & Cordeiro, M. N. D. (2019). Probing the environmental toxicity of deep eutectic solvents and their components: An in-silico modeling approach. *ACS Sustainable Chemistry & Engineering*, *7*(12), 10649-10660.

Sundar, S., Venkatachalam, G., & Kwon, S. J. (2018). Biosynthesis of copper oxide (CuO) nanowires and their use for the electrochemical sensing of dopamine. *Nanomaterials*, *8*(10), 823.

Majeed, A. M. A., Abd, A. N., Hussein, A. A., & Habubi, N. F. (2015). Fabrication and Characterization of Copper Oxide Nanoparticles/PSi Heterodiode, 57, 25–35.

Ali, E. M., Rasool, K. H., Abad, W. K., & Abd, A. N. (2021, July). Green Synthesis, Characterization and Antimicrobial activity of CuO nanoparticles (NPs) Derived from Hibiscus sabdariffa a plant and CuCl. In *Journal of Physics: Conference Series* (Vol. 1963, No. 1, p. 012092). IOP Publishing.

Muthuvel, A., Jothibas, M., & Manoharan, C. (2020). Synthesis of copper oxide nanoparticles by chemical and biogenic methods: photocatalytic degradation and in vitro antioxidant activity. *Nanotechnology for Environmental Engineering*, *5*, 1-19.

Jassim, A. M., Farhan, S. A., Salman, J. A., Khalaf, K. J., Al Marjani, M. F., & Mohammed, M. T. (2015). Study the antibacterial effect of bismuth oxide and tellurium nanoparticles. *Int j chem biol sci*, *1*(3), 81-84.

Apsana, G., George, P. P., Devanna, N., & Yuvasravana, R. (2018). Biomimetic synthesis and antibacterial properties of strontium oxide nanoparticles using Ocimum sanctum leaf extract. *Asian J. Pharm. Clin. Res*, *11*, 384-389.

Anbu, S., Hoffmann, S. H., Carniato, F., Kenning, L., Price, T. W., Prior, T. J., ... & Stasiuk, G. J. (2021). A Single-Pot Template Reaction Towards a Manganese-Based T1 Contrast Agent. Angewandte Chemie, 133(19), 10831-10839.

Kazemi, M., Akbari, A., Zarrinfar, H., Soleimanpour, S., Sabouri, Z., Khatami, M., & Darroudi, M. (2020). Evaluation of antifungal and photocatalytic activities of gelatin-stabilized selenium oxide nanoparticles. *Journal of Inorganic and Organometallic Polymers and Materials*, *30*, 3036-3044.

Khazaal, F. A., Kadhim, M. M., Husseein, H. F., Abbas, Z. M., SHamzah, M., Khudhair, I. A., ... & Saieed, H. S. (2020). Electronic transfers and (nlo) properties predicted by ab initio methods with prove experimentally. *NeuroQuantology*, *18*(1), 46.